LC-TH-2003-093
DESY-03-074
HD-THEP-03-29
hep-ph/0306247

Probing triple gauge couplings with transverse beam polarisation in $e^+e^- \to W^+W^-$

M. Diehl[1]

Deutsches Elektronen-Synchrotron DESY, 22603 Hamburg, Germany

O. Nachtmann[2] and F. Nagel[3]

Institut für Theoretische Physik, Philosophenweg 16, 69120 Heidelberg, Germany

Abstract

The prospects of measuring triple gauge couplings in W pair production at future linear colliders with transverse beam polarisation are studied. We consider CP conserving and CP violating couplings with both real and imaginary parts. The maximum achievable sensitivity in a simultaneous measurement of all couplings is determined using optimal observables, extending an earlier analysis for longitudinal beam polarisation. We find good sensitivity to the coupling $\mathrm{Im}(g_1^R + \kappa_R)$, which is not measurable with longitudinal polarisation. In contrast, for the real parts (including the CP violating couplings) the sensitivity is better if both beams are longitudinally polarised. We conclude that a comprehensive measurement of all triple gauge couplings requires both transverse and longitudinal beam polarisation.

[1]email: markus.diehl@desy.de
[2]email: O.Nachtmann@thphys.uni-heidelberg.de
[3]email: F.Nagel@thphys.uni-heidelberg.de

1 Introduction

Future linear e^+e^- colliders like TESLA [1] or CLIC [2] offer remarkable opportunities to probe the Standard Model (SM) and its numerous proposed extensions. The wide c.m. energy range from 90 GeV to 800 GeV or possibly 1 TeV at TESLA and from 500 GeV to 5 TeV at CLIC, the high integrated luminosities in the inverse attobarn region, the clean environment of e^+e^- collisions, and the possibility to use polarised beams allow for a variety of precision measurements of the electroweak interactions. Here we consider the triple gauge couplings (TGCs) γWW and ZWW.

The TGCs are interesting observables for several reasons: Firstly, the most general γWW and ZWW vertices contain altogether 14 complex parameters [3], six of them CP violating. In the SM the TGCs are predicted by the non-Abelian gauge symmetry, and only four CP conserving real couplings are non-zero at tree level. A variety of new physics effects can manifest itself by deviations from the SM predictions [4]. Secondly, in reactions where longitudinal W boson states are produced via TGCs the measurement of these couplings may provide information about the mechanism of electroweak symmetry breaking [5]. Thirdly, though no deviation from the SM has been found for the TGCs from LEP data [6], the bounds obtained are comparatively weak. The tightest bounds on the anomalous couplings, i.e. on the differences between a coupling and its SM value, are of order 0.05 for Δg_1^Z and λ_γ, of order 0.1 for $\Delta\kappa_\gamma$ and of order 0.1 to 0.6 for the real and imaginary parts of C and/or P violating couplings.[4] Moreover, many couplings, e.g. the imaginary parts of C and P conserving couplings, have been excluded from the analyses so far.

For various measurements at future colliders, longitudinal polarisation of one or both beams is expected to significantly improve the sensitivity, see e.g. [7]. A dedicated study of $e^-e^+ \to W^-W^+$ has been performed in [8]. Longitudinal beam polarisation indeed enhances the sensitivity to most TGCs. The linear combination of couplings $\mathrm{Im}(g_1^R + \kappa_R)$ can however not be measured from the normalised event distribution, unless the beam polarisation is *transverse*. Further information on this coupling is contained in the total event rate as discussed in [8], but the corresponding constraints depend on the values of all other couplings. Moreover, the total event rate is likely dominated by systematic errors, which we do not attempt to quantify here.

At present the physics case for transverse beam polarisation at a linear collider is being discussed [9, 10]. Once the planned degree of longitudinal polarisation is realised in experiment, viz. about $P_l^- = \pm 80\%$ for the electron and about $P_l^+ = \pm 60\%$ for the positron beam, the same degrees of transverse polarisation $P_t^\pm$ are considered to be feasible. Then the important question arises of how to distribute the available total luminosity among the different modes. Thus, the physics cases for the various polarisation modes must be studied.

The purpose of this paper is to analyse the gain or loss in sensitivity to all 28

[4]These numbers correspond to fits where all anomalous couplings except one are set to zero.

TGCs using transverse instead of longitudinal beam polarisation in the reaction $e^-e^+ \to W^-W^+ \to 4$ fermions. To this end we consider the full normalised event distribution. Our work is complementary to [11], where the total cross section for different W boson helicities as well as the left-right and transverse asymmetries—both integrated and as a function of the W production angle—were calculated for the same reaction, including order α corrections and bremsstrahlung. The sensitivity of the cross section and of various angular distributions in the final state was investigated in an early study of polarisation for LEP2 [12]. Only a restricted number of CP conserving form factors without imaginary parts was considered in these works. Here, in contrast, we determine the maximum sensitivity to the full set of parameters by means of optimal observables. The differential cross section for arbitrary polarisation can be written as a sum where the first term depends on $P_l^{\pm}$ and the second is proportional to the product $(P_t^- \cdot P_t^+)$, see (16) in [8]. Hence, there can be only effects of transverse polarisation if both beams are polarised and if both the electron and the positron spin vectors have a transverse component. In the following we consider only longitudinal *or* transverse polarisation, but no hybrid, though it is in general not excluded that the sensitivity of the differential cross section to some parameters can improve by considering more generic directions of the electron and positron spin vectors. Furthermore, we quantify the statement in [8] that the coupling $\mathrm{Im}(g_1^R + \kappa_R)$ is measurable with transverse polarisation.

The outline of this work is as follows: In Sect. 2 we summarise the results for the differential cross section with arbitrary beam polarisation using the notation of [8]. We repeat the definitions of the tensors, frames and angles in detail here, because they are crucial in the context of transverse polarisation. In Sect. 3 we recall the classification of the TGCs into four symmetry classes. We then show that this can be exploited to measure couplings of different symmetry classes independently with any type of beam polarisation (as it can be with longitudinal polarisation, see [8]). In Sect. 4 we make some general statements about the measurement of TGCs in W pair production with transverse beam polarisation. In Sect. 5 we present our numerical results. We give the minimum achievable errors on all 28 TGCs when they are measured simultaneously, i.e. none of them is assumed to be zero. These results are then compared to the propects of measurement with unpolarised beams and with longitudinal polarisation. In Sect. 6 we present our conclusions.

2 W pair production

In this section we introduce our notation and briefly review the results of [8] for the differential cross section of the process

$$e^-e^+ \longrightarrow W^-W^+ \longrightarrow (f_1\overline{f_2})(f_3\overline{f_4}), \tag{1}$$

where the final state fermions are leptons or quarks. All definitions and results of this section can be found in [8] and are repeated here only for the convenience of the reader.

As in [8] the process is calculated in the SM with the γWW and ZWW vertices replaced by their most general form allowed by Lorentz invariance. In particular, we use the fermion-boson vertices of the SM. We parameterise the γWW and ZWW vertices by the parameters g_1^V, κ_V, λ_V, g_4^V, g_5^V, $\tilde{\kappa}_V$, $\tilde{\lambda}_V$ with $V = \gamma$ or Z, see (2.4) in [3]. In the SM at tree level one has

$$g_1^V = 1, \quad \kappa_V = 1 \qquad (V = \gamma, Z), \tag{2}$$

and all other couplings are equal to zero. As usual we denote deviations from the SM values (2) by $\Delta g_1^V = g_1^V - 1$ and $\Delta\kappa_V = \kappa_V - 1$. It has been emphasised [14] that the following linear combinations of couplings, introduced in [3], can be measured with much smaller correlations:

$$\begin{aligned} g_1^L &= 4\sin^2\theta_W\, g_1^\gamma + (2 - 4\sin^2\theta_W)\,\xi\, g_1^Z, \\ g_1^R &= 4\sin^2\theta_W\, g_1^\gamma - 4\sin^2\theta_W\,\xi\, g_1^Z, \end{aligned} \tag{3}$$

where $\xi = s/(s - m_Z^2)$, and similarly for the other couplings. The L- and R-couplings respectively appear in the amplitudes for left- and right-handed initial e^-. We use the parameterisation (3) where appropriate.

Fig. 1 shows our definitions of the particle momenta and helicities. The production of the W bosons is described in the e^-e^+ c.m. frame. The coordinate axes are chosen such that the e^- momentum points in the positive z-direction and the y unit vector is given by $\hat{\boldsymbol{e}}_{\boldsymbol{y}} = (\mathbf{k}\times\mathbf{q})/|\mathbf{k}\times\mathbf{q}|$. At a given c.m. energy $\sqrt{s}$, a pure initial state of

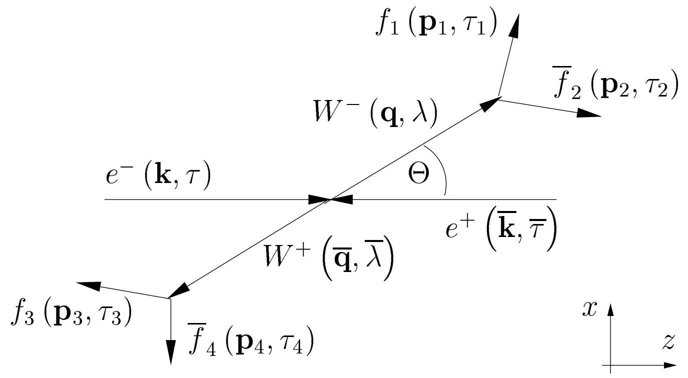

Figure 1: Momenta and helicities in the e^-e^+ c.m. frame.

e^- and e^+ with longitudinal polarisation can be uniquely specified by the e^- and e^+ helicities in the c.m. frame:

$$|\tau\overline{\tau}\rangle = |e^-(\mathbf{k}, \tau)e^+(\overline{\mathbf{k}}, \overline{\tau})\rangle \qquad (\tau, \overline{\tau} = \pm 1). \tag{4}$$

Here and in the following fermion helicity indices are normalised to 1. A mixed initial state with general polarisation is given by the operator

$$\boldsymbol{\rho} = \sum_{(\tau)} |\tau\overline{\tau}\rangle \rho_{(\tau\overline{\tau})(\tau'\overline{\tau}')} \langle\tau'\overline{\tau}'|, \tag{5}$$

where $\rho_{(\tau\overline{\tau})(\tau'\overline{\tau}')}$ is the spin density matrix of the combined e^-e^+ system and (τ) denotes summation over τ, $\overline{\tau}$, τ' and $\overline{\tau}'$. The matrix entries satisfy

$$\rho^*_{(\tau\overline{\tau})(\tau'\overline{\tau}')} = \rho_{(\tau'\overline{\tau}')(\tau\overline{\tau})}, \qquad\qquad \sum_{\tau,\overline{\tau}} \rho_{(\tau\overline{\tau})(\tau\overline{\tau})} = 1. \tag{6}$$

The differential cross section with the initial state $\boldsymbol{\rho}$ is given by the trace

$$\mathrm{d}\sigma|_\rho = \mathrm{tr}(\mathbf{d}\boldsymbol{\sigma}\boldsymbol{\rho}) = \sum_{(\tau)} \mathrm{d}\sigma_{(\tau'\overline{\tau}')(\tau\overline{\tau})}\, \rho_{(\tau\overline{\tau})(\tau'\overline{\tau}')}, \tag{7}$$

where $\mathbf{d}\boldsymbol{\sigma}$ is the operator

$$\mathbf{d}\boldsymbol{\sigma} = \sum_{(\tau)} |\tau'\overline{\tau}'\rangle \mathrm{d}\sigma_{(\tau'\overline{\tau}')(\tau\overline{\tau})} \langle\tau\overline{\tau}|. \tag{8}$$

Using the narrow-width approximation for the Ws, the matrix entries in (8) are

$$\mathrm{d}\sigma_{(\tau'\overline{\tau}')(\tau\overline{\tau})} \;=\; \frac{\beta}{(8\pi)^6 (m_W\Gamma_W)^2\, s} \sum_{(\lambda)} \mathrm{d}\mathcal{P}^{(\lambda\overline{\lambda})(\lambda'\overline{\lambda}')}_{(\tau'\overline{\tau}')(\tau\overline{\tau})}\, \mathrm{d}\mathcal{D}_{\lambda'\lambda}\, \mathrm{d}\overline{\mathcal{D}}_{\overline{\lambda}'\overline{\lambda}}\ . \tag{9}$$

Here m_W is the W boson mass, Γ_W its width, and $\beta = (1-4m_W^2/s)^{1/2}$ its velocity in the e^-e^+ c.m. frame. The sum (λ) runs over λ, λ', $\overline{\lambda}$ and $\overline{\lambda}'$. Denoting the transition operator by $\mathcal{T}$ the differential production tensor for the W pair is

$$\mathrm{d}\mathcal{P}^{(\lambda\overline{\lambda})(\lambda'\overline{\lambda}')}_{(\tau'\overline{\tau}')(\tau\overline{\tau})} = \mathrm{d}(\cos\Theta)\, \mathrm{d}\Phi\ \langle\lambda\overline{\lambda},\Theta|\mathcal{T}|\tau\overline{\tau}\rangle\ \langle\lambda'\overline{\lambda}',\Theta|\mathcal{T}|\tau'\overline{\tau}'\rangle^* \tag{10}$$

and the tensors of the W^- and W^+ decays in their respective c.m. frames are

$$\begin{aligned}
\mathrm{d}\mathcal{D}_{\lambda'\lambda} &= \mathrm{d}(\cos\vartheta)\, \mathrm{d}\varphi\ \langle f_1\overline{f_2}|\mathcal{T}|\lambda\rangle\ \langle f_1\overline{f_2}|\mathcal{T}|\lambda'\rangle^*, \\
\mathrm{d}\overline{\mathcal{D}}_{\overline{\lambda}'\overline{\lambda}} &= \mathrm{d}(\cos\overline{\vartheta})\, \mathrm{d}\overline{\varphi}\ \langle f_3\overline{f_4}|\mathcal{T}|\overline{\lambda}\rangle\ \langle f_3\overline{f_4}|\mathcal{T}|\overline{\lambda}'\rangle^*.
\end{aligned} \tag{11}$$

The matrix elements in (10) and (11) are given in [3]. The W bosons are produced by SM neutrino exchange in the t-channel, and by s-channel photon and Z production via the TGCs of the SM and the anomalous TGCs. We note that in our process there are possible effects of physics beyond the SM which cannot be parameterised in terms of TGCs, see e.g. [15]. For further discussion of this point we refer to [8].

The W helicity states occurring on the right-hand side of (10) are defined in the frame of Fig. 1. By Θ we denote the polar angle between the W^- and e^- momenta. Furthermore, we choose a fixed direction transverse to the beams in the laboratory. By Φ we denote the azimuthal angle between this fixed direction and the $e^-e^+ \to W^-W^+$ scattering plane (see Fig. 2(a)). The respective frames for the decay tensors (11) are defined by a rotation by Θ about the y-axis of the frame in Fig. 1 (such that the W^- momentum points in the new positive z-direction) and a subsequent rotation-free boost into the c.m. system of the corresponding W. The spherical coordinates in

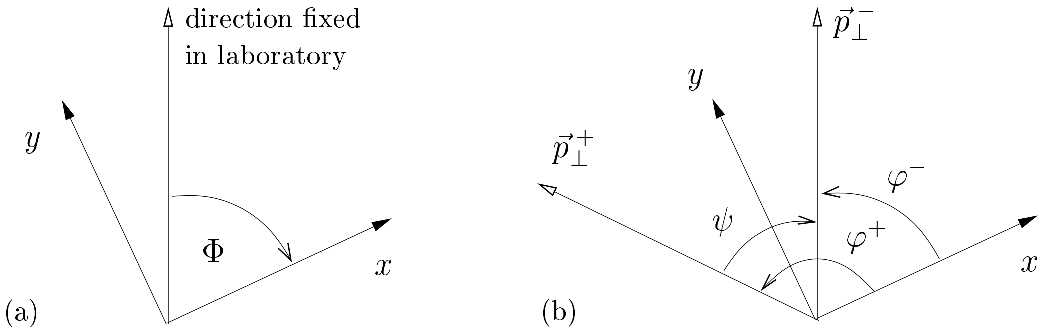

Figure 2: Definition of azimuthal angles. The x-axis points in the direction of $\mathbf{q}_\perp$.

(11) are those of the f_1 and $\overline{f_4}$ momentum directions, respectively. In its rest frame, the quantum state of a W boson is determined by its polarisation. In the narrow-width approximation the intermediate Ws are treated as on-shell, so that we can take as basis the eigenstates of the spin operator S_z with the three eigenvalues $\lambda = \pm 1, 0$.

Subsequently, we set the electron mass to zero. Since we assume SM couplings for the electron-boson vertices we have the relations

$$\mathrm{d}\sigma_{(\tau'\overline{\tau}')(\tau\overline{\tau})} = 0 \qquad\qquad \text{for } \tau = \overline{\tau} \text{ or } \tau' = \overline{\tau}'. \tag{12}$$

Assuming the initial beams to be uncorrelated their spin density matrix factorises:

$$\rho_{(\tau\overline{\tau})(\tau'\overline{\tau}')} = \rho_{\tau\tau'}\overline{\rho}_{\overline{\tau}\,\overline{\tau}'} \;\; , \tag{13}$$

where $\rho_{\tau\tau'}$ and $\overline{\rho}_{\overline{\tau}\,\overline{\tau}'}$ are the two Hermitian and normalised spin density matrices of e^- and e^+, respectively. As in [8] we parameterise these matrices by

$$\rho_{\tau\tau'} = \frac{1}{2}\left(\mathbb{1} + \vec{p}^{\,-}\cdot\vec{\sigma}\right)_{\tau\tau'} , \qquad \overline{\rho}_{\overline{\tau}\,\overline{\tau}'} = \frac{1}{2}\left(\mathbb{1} - \vec{p}^{\,+}\cdot\vec{\sigma}^{\,*}\right)_{\overline{\tau}\,\overline{\tau}'} \tag{14}$$

with

$$\vec{p}^{\,\pm} = P_t^\pm \begin{pmatrix} \cos\varphi^\pm \\ \sin\varphi^\pm \\ 0 \end{pmatrix} + P_l^\pm \begin{pmatrix} 0 \\ 0 \\ \mp 1 \end{pmatrix} . \tag{15}$$

The range of the azimuthal angles is $0 \le \varphi^\pm < 2\pi$. The components of $\vec{\sigma}$ are the Pauli matrices. The degrees $P_t^\pm$ of transverse and $P_l^\pm$ of longitudinal polarisation obey the relations $(P_t^\pm)^2 + (P_l^\pm)^2 \le 1$ and $P_t^\pm \ge 0$. The components of $\vec{p}^{\,\pm}$ in (15) refer to the frame of Fig. 1. The relative azimuthal angle $\psi = \varphi^- - \varphi^+$ between $\vec{p}^{\,-}$ and $\vec{p}^{\,+}$ is fixed by the experimental conditions, whereas the azimuthal angles φ^- of $\vec{p}^{\,-}$ and φ^+ of $\vec{p}^{\,+}$ in the system of Fig. 1 depend on the final state (see Fig. 2(b)). For the case where $P_t^- \neq 0$ we choose the transverse part of the vector $\vec{p}^{\,-}$ as fixed direction in the laboratory. Then we have $\Phi = -\varphi^-$. With these conventions the differential cross section for arbitrary beam polarisation is

$$
\begin{aligned}
\mathrm{d}\sigma|_\rho \;=\; & \frac{1}{4}\Big\{(1+P_l^-)(1-P_l^+)\,\mathrm{d}\sigma_{(+-)(+-)} \\
& + (1-P_l^-)(1+P_l^+)\,\mathrm{d}\sigma_{(-+)(-+)} \\
& - 2P_t^-P_t^+\Big[\mathrm{Re}\,\mathrm{d}\sigma_{(+-)(-+)}\,\cos(\psi+2\Phi) \\
& \qquad + \mathrm{Im}\,\mathrm{d}\sigma_{(+-)(-+)}\,\sin(\psi+2\Phi)\Big]\Big\}.
\end{aligned}
\tag{16}
$$

In this formula the azimuthal angle Φ occurs only in the arguments of the two trigonometric functions.

3 CP and $CP\tilde{T}$

As is well-known [3] the real and the imaginary parts of the couplings g_1, κ, λ, and g_5 are CP conserving, whereas those of g_4, $\tilde{\kappa}$, and $\tilde{\lambda}$ are CP violating. Here CP denotes the combined discrete symmetry of charge conjugation and parity transformation. Furthermore, the real parts of the couplings are $CP\tilde{T}$ conserving, whereas their imaginary parts are $CP\tilde{T}$ violating, where $\tilde{T}$ denotes "naïve time reversal", i.e. the reversal of all particle momenta and spins without the interchange of initial and final state. Hence the TGCs can be classified as follows [14, 16]:

(a) CP and $CP\tilde{T}$ conserving,
(b) CP conserving and $CP\tilde{T}$ violating,
(c) CP violating and $CP\tilde{T}$ conserving,
(d) CP and $CP\tilde{T}$ violating.

Since the interactions are invariant under rotations we can, instead of a pure $CP\tilde{T}$ transformation, equally well consider $RCP\tilde{T}$, i.e. $CP\tilde{T}$ followed by a rotation R by 180 degrees around $\hat{\boldsymbol{e}}_{\boldsymbol{y}}$. Notice that this differs from the definition of R in Sect. 3.3 of [8] where the rotation axis is $(\mathbf{k}\times\vec{p}^{\,-})$. More detail is given in Appendices A and B.

When measured with an appropriate set of observables [14], couplings from different symmetry groups have uncorrelated statistical errors (to leading order in the anomalous couplings), provided that phase space cuts, detector acceptance and the initial state are invariant under CP and $RCP\tilde{T}$. As mentioned in [8], CP and $RCP\tilde{T}$ violating effects from the initial state in $e^-e^+\to W^-W^+$ are suppressed by (m_e/m_W) with transverse beam polarisation and by $(m_e/m_W)^2$ with longitudinal polarisation or unpolarised beams. Consequently, these effects vanish in the limit $m_e\to 0$ for an arbitrary spin density matrix $\boldsymbol{\rho}$. This means that, although the initial state is *not* invariant under CP and $RCP\tilde{T}$, it is *effectively* invariant for our reaction in the $m_e\to 0$ limit. Let us make this more explicit.

Both the CP and the $RCP\tilde{T}$ transformation of the initial state leave the particle momenta unchanged and correspond to the following transformation of the spin density matrix:

$$\rho_{(\tau\overline{\tau})(\tau'\overline{\tau}')} \quad \xrightarrow{CP,\, RCP\tilde{T}} \quad \rho_{(\overline{\sigma}\sigma)(\overline{\sigma}'\sigma')}\ \epsilon_{\overline{\sigma}\overline{\tau}}\ \epsilon_{\sigma\tau}\ \epsilon_{\overline{\sigma}'\overline{\tau}'}\ \epsilon_{\sigma'\tau'}\ , \tag{17}$$

where

$$\epsilon = \begin{pmatrix} 0 & 1 \\ -1 & 0 \end{pmatrix}. \tag{18}$$

This transformation rule is derived in Appendix B. Thus invariance of the spin density matrix under either of the two symmetries requires

$$\rho_{(\tau\overline{\tau})(\tau'\overline{\tau}')} = \rho_{(\overline{\sigma}\sigma)(\overline{\sigma}'\sigma')}\ \epsilon_{\overline{\sigma}\overline{\tau}}\ \epsilon_{\sigma\tau}\ \epsilon_{\overline{\sigma}'\overline{\tau}'}\ \epsilon_{\sigma'\tau'}\ . \tag{19}$$

If the spin density matrix factorises as in (13) we find

$$\rho_{\tau\tau'} = \left(\epsilon^{\mathrm{T}}\overline{\rho}\,\epsilon\right)_{\tau\tau'}. \tag{20}$$

In our parameterisation the spin density matrices are explicitly given by

$$\rho_{\tau\tau'} \;=\; \frac{1}{2}\begin{pmatrix} (1+P_l^-) & P_t^- e^{-\mathrm{i}\varphi^-} \\ P_t^- e^{\mathrm{i}\varphi^-} & (1-P_l^-) \end{pmatrix}_{\tau\tau'}, \tag{21}$$

$$\overline{\rho}_{\overline{\tau}\overline{\tau}'} \;=\; \frac{1}{2}\begin{pmatrix} (1+P_l^+) & -P_t^+ e^{\mathrm{i}\varphi^+} \\ -P_t^+ e^{-\mathrm{i}\varphi^+} & (1-P_l^+) \end{pmatrix}_{\overline{\tau}\overline{\tau}'}. \tag{22}$$

The requirement (20) thus reads

$$\rho_{\tau\tau'} \;=\; \frac{1}{2}\begin{pmatrix} (1-P_l^+) & P_t^+ e^{-\mathrm{i}\varphi^+} \\ P_t^+ e^{\mathrm{i}\varphi^+} & (1+P_l^+) \end{pmatrix}_{\tau\tau'}, \tag{23}$$

which leads to the following conditions on the polarisation parameters:

$$P_l^- = -P_l^+, \qquad P_t^- = P_t^+, \qquad \varphi^- = \varphi^+. \tag{24}$$

If we do not demand CP or $RCP\tilde{T}$ invariance of the full spin density matrix but only consider those matrix entries that give non-vanishing amplitudes we find, instead of (19):

$$\tilde{\rho}_{(\tau\overline{\tau})(\tau'\overline{\tau}')} = \tilde{\rho}_{(\overline{\sigma}\sigma)(\overline{\sigma}'\sigma')}\ \epsilon_{\overline{\sigma}\overline{\tau}}\ \epsilon_{\sigma\tau}\ \epsilon_{\overline{\sigma}'\overline{\tau}'}\ \epsilon_{\sigma'\tau'}\ , \tag{25}$$

with a "reduced" spin density matrix

$$\tilde{\rho}_{(\tau\overline{\tau})(\tau'\overline{\tau}')} = \begin{cases} \rho_{(\tau\overline{\tau})(\tau'\overline{\tau}')} & \text{for } \overline{\tau} = -\tau \text{ and } \overline{\tau}' = -\tau' \\ 0 & \text{else.} \end{cases} \tag{26}$$

Inserting this definition into (25) we find that the condition for CP or $RCP\tilde{T}$ invariance is trivially fulfilled. Under the assumption that only amplitudes with $\overline{\tau} = -\tau$ contribute to the differential cross section and that the factorisation (13) is possible, no condition has therefore to be imposed on $P_l^{\pm}$, $P_t^{\pm}$ or $\varphi^{\pm}$ to guarantee absence of CP or $RCP\tilde{T}$ violation in the initial state. Any violation of CP or $CP\tilde{T}$ is then due to the interaction.

4 Sensitivity to couplings

To investigate the prospects of measuring anomalous TGCs in the process (1) with transverse beam polarisation we use optimal observables [17, 14]. In the limit of small couplings, the statistical errors on the couplings determined with this method are minimal compared with any other set of observables. To be more precise, these observables minimise the errors for a given *normalised* event distribution. The integrated cross section still contains complementary information on the couplings. For more details concerning optimal observables we refer to Sect. 3 in [8] where they are applied to the same reaction with longitudinal beam polarisation. Before listing our results in Sect. 5 we now discuss some aspects of transverse polarisation in the context of the process (1).

Looking at the differential cross section (16) we see that a change in ψ by $\Delta\psi$ is equivalent to a rotation of the whole event distribution about the beam axis by $\Delta\Phi = \Delta\psi/2$. It neither changes the shape of the distribution nor the total event rate. The sensitivity to the TGCs thus does not depend on ψ. Integrating the differential cross section over Φ, the terms proportional to $\cos(\psi + 2\Phi)$ and $\sin(\psi + 2\Phi)$ in (16) vanish. The total cross section is hence independent of P_t^-, P_t^+ and ψ. Therefore, in absence of longitudinal polarisation, the total cross section with transversely polarised beams equals that with unpolarised beams. This cross section is shown in Fig. 4 of [8] for the SM and with various anomalous TGCs. Some other quantities required for the optimal observable method are also the same for pure transverse polarisation and for unpolarised beams. These are in particular the total cross section in the SM σ_0, the expectation values of the optimal observables in the SM $E_0[\mathcal{O}_i]$, and the normalised second-order part of the total cross section $\hat{\sigma}_{2ij}$, see (26) and (36) in [8].

As seen in Sect. 3, the initial state is not invariant under the discrete symmetries CP and $RCP\tilde{T}$ for generic beam polarisation. It is however *effectively* invariant if the electron mass is neglected, because then only a subset of helicity amplitudes is non-zero. Hence the results of Sect. 3.3 in [8] apply, i.e. a given optimal observable is sensitive only to couplings of the same symmetry class (a), (b), (c), or (d). Measurement errors on couplings of different symmetry classes are not correlated to leading order in the anomalous couplings. Furthermore, the first-order terms in the integrated cross section vanish except for symmetry (a), where only the g_5^R-term is zero.

5 Numerical results

In this section we present our results for the sensitivity to anomalous TGCs in the reaction (1) with transverse beam polarisations $P_t^- = 80\%$ of the electron and $P_t^+ = 60\%$ of the positron beam. As in [8] we consider only events where one W boson decays into a quark-antiquark pair and the other one into $e\nu$ and $\mu\nu$. These decay channels have a branching ratio of altogether 8/27. We assume that the two jets of the hadronic W decay cannot be identified as originating from the up- and down-type (anti)quark. This must be taken into account in the definition of the optimal observables as explained in [16]. To measure the coupling parameters these observables have the maximum sensitivity that one can obtain from the sum of the event distributions corresponding to the two final states.

For the masses of the W and Z we use $m_W = 80.42$ GeV and $m_Z = 91.19$ GeV [13] and define the weak mixing angle by $\sin^2\theta_W = 1 - m_W^2/m_Z^2$. For the total event rate N with transverse beam polarisation we use the values listed in Table 3 of [8], viz. 1.14×10^6 for a c.m. energy of 500 GeV and 1.19×10^6 for 800 GeV. These values are computed for an effective electromagnetic coupling $\alpha = 1/128$ and integrated luminosities of 500 fb^{-1} at 500 GeV and 1 ab^{-1} at 800 GeV.

In Tables 1 to 4 we give the standard deviations $\delta h_i = [V(h)_{ii}]^{1/2}$ for the couplings of symmetry classes (a) to (d), as well as the correlation matrices

$$W(h)_{ij} = \frac{V(h)_{ij}}{\sqrt{V(h)_{ii}V(h)_{jj}}}, \tag{27}$$

where $V(h)_{ij}$ is the covariance matrix of the couplings in the L-R-parameterisation (3). V and W are evaluated with zero anomalous couplings, and errors on couplings in different symmetry classes are uncorrelated to this accuracy. The δh_i are the errors obtained without assuming any other anomalous coupling to be zero. For symmetry (b) we use the linear combinations $\tilde{h}_\pm = \mathrm{Im}(g_1^R \pm \kappa_R)/\sqrt{2}$ instead of $\mathrm{Im}\, g_1^R$ and $\mathrm{Im}\, \kappa_R$ to allow for better comparison with the results for unpolarised beams and longitudinal polarisation, where the normalised event distribution is sensitive to $\tilde{h}_-$, but not to $\tilde{h}_+$. The range of the δh_i within each symmetry class is from about 5×10^{-4} to about 5×10^{-3}. Notice that both $\tilde{h}_+$ and $\tilde{h}_-$ are measurable with an error of about 3.5×10^{-3} using transverse polarisation. This confirms and makes quantitive the result of [8] that one is indeed sensitive to $\tilde{h}_+$ with transverse polarisation. Also the sensitivity to $\tilde{h}_-$ is significantly better than with unpolarised beams, where the error is about 10^{-2}. The high correlation between $\tilde{h}_+$ and $\tilde{h}_-$ however suggests that the parameterisation with $\mathrm{Im}\, g_1^R$ and $\mathrm{Im}\, \kappa_R$ is preferable in an analysis of the data from transverse polarisation (whereas it is inadequate with longitudinal polarisation or unpolarised beams). The gain by different types of polarisation at 500 GeV can be seen from Tables 5 to 8 for the four symmetry classes. In Tables 9 to 12 the same is shown for 800 GeV. To allow for better comparison with other studies we use the photon- and Z-couplings for the results of symmetries (a), (c) and (d) instead of the L-and R-couplings, although the latter are in general less correlated. We use however the L-R-couplings for symmetry (b), where only one coupling is unmeasurable without transverse beam polarisation. In the γ-Z-parameterisation, four couplings, $\mathrm{Im}\, g_1^\gamma$, $\mathrm{Im}\, g_1^Z$, $\mathrm{Im}\, \kappa_\gamma$ and $\mathrm{Im}\, \kappa_Z$, are not measurable in the absence of transverse polarisation, because their linear combination $\tilde{h}_+$ is not. In the unpolarised case the assumed luminosity is 500 fb^{-1} at 500 GeV and 1 ab^{-1} at 800 GeV. The same values are used for the results with transverse polarisation in the fourth row of each table. For the results with longitudinal e^- polarisation in the second row we assume that one half of the luminosity is used for $P_l^- = +80\%$ and the other half for $P_l^- = -80\%$. Similarly, for the results in the third row with additional longitudinal e^+ polarisation we assume that the total luminosity is equally distributed among the settings with $(P_l^-, P_l^+) = (+80\%, -60\%)$ and $(-80\%, +60\%)$. For each of rows number two and three, the results from the two settings are combined in the conventional way, i.e. we take the two covariance matrices V_1 and V_2, and compute the matrix

$$V = \left(V_1^{-1} + V_2^{-1}\right)^{-1}. \tag{28}$$

This is the covariance matrix on the couplings if they are determined by a weighted average from two individual measurements. V_1, V_2 and V are 8×8 matrices for symmetry class (a) and 6×6 matrices for symmetry classes (c) and (d), whereas in the case of symmetry class (b) they are 7×7 matrices since the coupling $\tilde{h}_+$ is excluded. The square roots of the diagonal elements of V are then the 1σ-errors, which we list in the second and third rows of Tables 5 to 12.

For a c.m. energy of 500 GeV the errors with unpolarised beams are between 10^{-3} and 10^{-2} in the γ-Z-parameterisation (see Tables 5, 7, and 8). All errors (with or without polarisation) are smaller at 800 GeV (see Tables 9 to 12), notably for $\mathrm{Re}\, \Delta\kappa_\gamma$ and $\mathrm{Im}\, \lambda_R$. For both c.m. energies the errors on all couplings in the γ-Z-parameterisation are about a factor 2 smaller with longitudinal e^- polarisation and unpolarised e^+ beam compared to the case where both beams are unpolarised. With additional longitudinal e^+ polarisation this factor is between 3 and 4 for all couplings, except for $\mathrm{Re}\, \Delta\kappa_Z$ at 800 GeV where it is 4.7. If both beams have transverse polarisation, the errors on most couplings are approximately of the same size as in the situation where only the e^- beam has longitudinal polarisation. Only for $\mathrm{Re}\, \lambda_\gamma$, $\mathrm{Re}\, \lambda_Z$, $\mathrm{Re}\, \tilde{\lambda}_\gamma$ and $\mathrm{Re}\, \tilde{\lambda}_Z$ are they smaller, viz. they are of the same size as with both beams longitudinally polarised. This is true for both energies. If electron as well as positron polarisation is available we thus conclude that, regarding the 1σ-standard deviations on the TGCs (without assuming any coupling to be zero) *longitudinal* polarisation is the preferable choice, except for $\tilde{h}_+$. We emphasize that we are better with longitudinal polarisation also for the CP violating couplings $\mathrm{Re}\, g_4^V$, $\mathrm{Re}\, \tilde{\lambda}_V$ and $\mathrm{Re}\, \tilde{\kappa}_V$ with $V = \gamma$ or Z.

Furthermore, we analyse how correlations between couplings depend on beam polarisation. Given the large number of parameters, small correlations are highly desirable. For brevity we do not present the full correlation matrices here for all different types of polarisation but only give the average over the absolute values of the off-diagonal elements in the correlation matrices (see Table 13). Furthermore, we restrict ourselves to symmetry (a) and a c.m. energy of 500 GeV.

Apart from the average over all 28 matrix entries we list the averages over the correlations between L-couplings, between R-couplings and those between one L- and one R-coupling. We see that no type of polarisation changes the average correlation between two L-couplings significantly. The average correlation between the R-couplings is most advantageous for transverse polarisation (26%), whereas in the other cases it ranges from 37% to 42%. On the other hand the L-couplings are hardly correlated with the R-couplings for longitudinal polarisation of e^- and e^+ (2%). This deteriorates with transverse polarisation, but the correlations remain very small (8%). Altogether, regarding the size of the correlations there is no strong argument to prefer one type of polarisation or the other.

Finally, we remark that the sensitivity to TGCs in our reaction has been analysed in [18] for unpolarised beams and for longitudinal polarisation. A maximum number of five CP conserving and four CP violating couplings was considered, but no imaginary parts were included (see Tables 5 and 6 of [18]). The author used a spin density matrix method where statistical errors are not necessarily optimal. A direct comparison with our results is however not possible. On the one hand the multi-parameter analysis of [18] includes beamstrahlung, initial state radiation and non-resonant diagrams. For the single parameter fits the full background calculated with PYTHIA and also detector acceptance is included. On the other hand only a restricted number of couplings is considered. An analysis using optimal observables with a full detector simulation and all 28 couplings would be desirable for unpolarised beams and both types of polarisation. This is however beyond the scope of our present work.

6 Conclusions

We have studied the prospects of measuring TGCs at a future linear collider in W pair production with transverse beam polarisation. Effects due to transverse polarisation can only occur if both beams are polarised and if both spins have a transverse component. The classification of the TGCs into four groups according to their properties under the discrete symmetries CP and $CP\tilde{T}$ remains valid in the case of transverse polarisation, neglecting effects which are at most $O(m_e/m_W)$. Using optimal observables these four groups of parameters can be measured without statistical correlation. Within each group, the errors on TGCs are correlated. We have given the errors and correlation matrices for a c.m. energy of 500 GeV with transverse polarisation of the electron ($P_t^- = 80\%$) and the positron beam ($P_t^+ = 60\%$) in the parameterisation with L- and R-couplings. The errors range from about 5×10^{-4} to about 5×10^{-3}. Moreover, we have compared the errors—mainly in the γ-Z-parameterisation—for transverse polarisation with those for unpolarised beams and with those for one or both beams longitudinally polarised. For most couplings the errors obtainable with

Table 1: Errors δh in units of 10^{-3} on the couplings of symmetry (a) (see Sect. 3) in the presence of all anomalous couplings, and correlation matrix $W(h)$ at $\sqrt{s} = 500$ GeV with transverse beam polarisation $(P_t^-, P_t^+) = (80\%, 60\%)$.

h	$\delta h \times 10^3$	$\mathrm{Re}\,\Delta g_1^L$	$\mathrm{Re}\,\Delta\kappa_L$	$\mathrm{Re}\,\lambda_L$	$\mathrm{Re}\,g_5^L$	$\mathrm{Re}\,\Delta g_1^R$	$\mathrm{Re}\,\Delta\kappa_R$	$\mathrm{Re}\,\lambda_R$	$\mathrm{Re}\,g_5^R$
$\mathrm{Re}\,\Delta g_1^L$	2.5	1	−0.58	−0.36	0.17	−0.068	0.18	−0.011	0.11
$\mathrm{Re}\,\Delta\kappa_L$	0.72		1	0.077	0.013	0.075	−0.46	0.023	−0.014
$\mathrm{Re}\,\lambda_L$	0.58			1	−0.011	0.053	−0.0040	0.029	0.045
$\mathrm{Re}\,g_5^L$	2.0				1	−0.14	−0.0027	−0.038	0.085
$\mathrm{Re}\,\Delta g_1^R$	4.2					1	−0.56	−0.41	0.35
$\mathrm{Re}\,\Delta\kappa_R$	1.2						1	0.075	−0.086
$\mathrm{Re}\,\lambda_R$	0.99							1	−0.066
$\mathrm{Re}\,g_5^R$	3.5								1

transverse polarisation are of the same order as with longitudinal e^- polarisation and unpolarised e^+ beam. If one has both beams polarised and can choose between longitudinal or transverse polarisation it is therefore advantageous to use longitudinal polarisation, except for the measurement of $\tilde{h}_+$. For the real parts of the couplings, the only advantage of transverse polarisation we found is that the average correlation among R-couplings is slightly reduced. The coupling $\tilde{h}_+$, however, is unmeasurable from the normalised event distribution with longitudinal polarisation, but it can be measured with an error of 3.2×10^{-3} using transverse polarisation. This suggests to use some fraction of the total luminosity to run the collider in this mode in order to get a comprehensive measurement of all TGCs. The required luminosity for a certain desired value of the statistical error on $\mathrm{Im}(g_1^R + \kappa_R)/\sqrt{2}$ can be easily calculated by applying the corresponding statistical factor.

Acknowledgements

The authors are grateful to P. Bock and G. Moortgat-Pick for useful remarks. This work was supported by the German Bundesministerium für Bildung und Forschung, project no. 05HT9HVA3, and the Deutsche Forschungsgemeinschaft with the Graduiertenkolleg "Physikalische Systeme mit vielen Freiheitsgraden" in Heidelberg.

Table 2: Same as Table 1, but for symmetry (b). We use the abbreviations $\tilde{h}_{\pm} = \mathrm{Im}(g_1^R \pm \kappa_R)/\sqrt{2}$.

h	$\delta h \times 10^3$	$\mathrm{Im}\, g_1^L$	$\mathrm{Im}\, \kappa_L$	$\mathrm{Im}\, \lambda_L$	$\mathrm{Im}\, g_5^L$	$\tilde{h}_-$	$\tilde{h}_+$	$\mathrm{Im}\, \lambda_R$	$\mathrm{Im}\, g_5^R$
$\mathrm{Im}\, g_1^L$	2.6	1	−0.63	−0.49	−0.20	0.050	−0.037	0.061	0.028
$\mathrm{Im}\, \kappa_L$	1.2		1	0.19	0.14	−0.072	0.051	−0.029	0.22
$\mathrm{Im}\, \lambda_L$	0.46			1	0.015	0.024	0.048	−0.063	−0.089
$\mathrm{Im}\, g_5^L$	2.0				1	−0.063	−0.053	0.10	0.18
$\tilde{h}_-$	3.7					1	0.81	−0.39	0.16
$\tilde{h}_+$	3.2						1	−0.39	0.11
$\mathrm{Im}\, \lambda_R$	0.98							1	−0.0041
$\mathrm{Im}\, g_5^R$	4.4								1

Table 3: Same as Table 1, but for symmetry (c).

h	$\delta h \times 10^3$	$\mathrm{Re}\, g_4^L$	$\mathrm{Re}\, \tilde{\lambda}_L$	$\mathrm{Re}\, \tilde{\kappa}_L$	$\mathrm{Re}\, g_4^R$	$\mathrm{Re}\, \tilde{\lambda}_R$	$\mathrm{Re}\, \tilde{\kappa}_R$
$\mathrm{Re}\, g_4^L$	2.4	1	−0.0082	−0.50	−0.072	−0.079	0.084
$\mathrm{Re}\, \tilde{\lambda}_L$	0.58		1	0.30	0.022	0.030	−0.074
$\mathrm{Re}\, \tilde{\kappa}_L$	2.6			1	0.090	0.056	0.063
$\mathrm{Re}\, g_4^R$	3.9				1	−0.013	−0.11
$\mathrm{Re}\, \tilde{\lambda}_R$	0.99					1	0.41
$\mathrm{Re}\, \tilde{\kappa}_R$	4.1						1

Table 4: Same as Table 1, but for symmetry (d).

h	$\delta h \times 10^3$	$\mathrm{Im}\, g_4^L$	$\mathrm{Im}\, \tilde{\lambda}_L$	$\mathrm{Im}\, \tilde{\kappa}_L$	$\mathrm{Im}\, g_4^R$	$\mathrm{Im}\, \tilde{\lambda}_R$	$\mathrm{Im}\, \tilde{\kappa}_R$
$\mathrm{Im}\, g_4^L$	1.8	1	0.0044	0.19	0.11	0.086	−0.0072
$\mathrm{Im}\, \tilde{\lambda}_L$	0.45		1	0.51	−0.10	−0.056	−0.022
$\mathrm{Im}\, \tilde{\kappa}_L$	1.9			1	−0.18	−0.047	0.0037
$\mathrm{Im}\, g_4^R$	3.6				1	−0.021	−0.32
$\mathrm{Im}\, \tilde{\lambda}_R$	0.97					1	0.43
$\mathrm{Im}\, \tilde{\kappa}_R$	3.7						1

Table 5: Errors δh in units of 10^{-3} on the couplings of symmetry (a) in the presence of all anomalous couplings at $\sqrt{s} = 500$ GeV, with unpolarised beams and with different beam polarisations.

	$\mathrm{Re}\,\Delta g_1^\gamma$	$\mathrm{Re}\,\Delta g_1^Z$	$\mathrm{Re}\,\Delta\kappa_\gamma$	$\mathrm{Re}\,\Delta\kappa_Z$	$\mathrm{Re}\,\lambda_\gamma$	$\mathrm{Re}\,\lambda_Z$	$\mathrm{Re}\,g_5^\gamma$	$\mathrm{Re}\,g_5^Z$
no polarisation	6.5	5.2	1.3	1.4	2.3	1.8	4.4	3.3
$(P_l^-, P_l^+) = (\mp 80\%, 0)$	3.2	2.6	0.61	0.58	1.1	0.86	2.2	1.7
$(P_l^-, P_l^+) = (\mp 80\%, \pm 60\%)$	1.9	1.6	0.40	0.36	0.62	0.50	1.4	1.1
$(P_t^-, P_t^+) = (80\%, 60\%)$	2.8	2.4	0.69	0.82	0.69	0.55	2.5	1.9

Table 6: Same as Table 5, but for symmetry (b) and with the L-R-parameterisation. We write again $\tilde{h}_\pm = \mathrm{Im}(g_1^R \pm \kappa_R)/\sqrt{2}$. Using this parameterisation, a maximum number of couplings can be measured without transverse beam polarisation. In the γ-Z-parameterisation, the four couplings $\mathrm{Im}\,g_1^\gamma$, $\mathrm{Im}\,g_1^Z$, $\mathrm{Im}\,\kappa_\gamma$ and $\mathrm{Im}\,\kappa_Z$ are not measurable without transverse polarisation.

	$\mathrm{Im}\,g_1^L$	$\mathrm{Im}\,\kappa_L$	$\mathrm{Im}\,\lambda_L$	$\mathrm{Im}\,g_5^L$	$\tilde{h}_-$	$\tilde{h}_+$	$\mathrm{Im}\,\lambda_R$	$\mathrm{Im}\,g_5^R$
no polarisation	2.7	1.7	0.48	2.5	11	—	3.1	17
$(P_l^-, P_l^+) = (\mp 80\%, 0)$	2.6	1.2	0.45	2.0	4.5	—	1.4	4.3
$(P_l^-, P_l^+) = (\mp 80\%, \pm 60\%)$	2.1	0.95	0.37	1.6	2.5	—	0.75	2.3
$(P_t^-, P_t^+) = (80\%, 60\%)$	2.6	1.2	0.46	2.0	3.7	3.2	0.98	4.4

Table 7: Same as Table 5, but for symmetry (c).

	$\mathrm{Re}\,g_4^\gamma$	$\mathrm{Re}\,g_4^Z$	$\mathrm{Re}\,\tilde{\lambda}_\gamma$	$\mathrm{Re}\,\tilde{\lambda}_Z$	$\mathrm{Re}\,\tilde{\kappa}_\gamma$	$\mathrm{Re}\,\tilde{\kappa}_Z$
no polarisation	6.2	5.1	2.4	1.9	7.3	5.4
$(P_l^-, P_l^+) = (\mp 80\%, 0)$	3.0	2.5	1.1	0.90	3.4	2.7
$(P_l^-, P_l^+) = (\mp 80\%, \pm 60\%)$	1.8	1.5	0.64	0.52	2.1	1.7
$(P_t^-, P_t^+) = (80\%, 60\%)$	2.7	2.3	0.69	0.55	2.9	2.3

Table 8: Same as Table 5, but for symmetry (d).

	$\mathrm{Im}\,g_4^\gamma$	$\mathrm{Im}\,g_4^Z$	$\mathrm{Im}\,\tilde{\lambda}_\gamma$	$\mathrm{Im}\,\tilde{\lambda}_Z$	$\mathrm{Im}\,\tilde{\kappa}_\gamma$	$\mathrm{Im}\,\tilde{\kappa}_Z$
no polarisation	5.1	3.6	1.8	1.4	5.6	4.2
$(P_l^-, P_l^+) = (\mp 80\%, 0)$	2.3	1.8	0.84	0.68	2.7	2.1
$(P_l^-, P_l^+) = (\mp 80\%, \pm 60\%)$	1.4	1.1	0.48	0.39	1.6	1.3
$(P_t^-, P_t^+) = (80\%, 60\%)$	2.5	1.8	0.63	0.53	2.5	2.0

Table 9: Same as Table 5, but for $\sqrt{s} = 800$ GeV.

	$\mathrm{Re}\,\Delta g_1^\gamma$	$\mathrm{Re}\,\Delta g_1^Z$	$\mathrm{Re}\,\Delta\kappa_\gamma$	$\mathrm{Re}\,\Delta\kappa_Z$	$\mathrm{Re}\,\lambda_\gamma$	$\mathrm{Re}\,\lambda_Z$	$\mathrm{Re}\,g_5^\gamma$	$\mathrm{Re}\,g_5^Z$
no polarisation	4.0	3.2	0.47	0.58	1.1	0.90	3.1	2.5
$(P_l^-, P_l^+) = (\mp 80\%, 0)$	1.9	1.6	0.21	0.21	0.53	0.43	1.6	1.3
$(P_l^-, P_l^+) = (\mp 80\%, \pm 60\%)$	1.1	0.97	0.14	0.13	0.29	0.24	0.97	0.82
$(P_t^-, P_t^+) = (80\%, 60\%)$	1.8	1.5	0.27	0.35	0.28	0.23	1.7	1.3

Table 10: Same as Table 6, but for $\sqrt{s} = 800$ GeV.

	$\mathrm{Im}\,g_1^L$	$\mathrm{Im}\,\kappa_L$	$\mathrm{Im}\,\lambda_L$	$\mathrm{Im}\,g_5^L$	$\tilde{h}_-$	$\tilde{h}_+$	$\mathrm{Im}\,\lambda_R$	$\mathrm{Im}\,g_5^R$
no polarisation	1.5	0.74	0.18	1.5	6.0	—	1.2	9.0
$(P_l^-, P_l^+) = (\mp 80\%, 0)$	1.5	0.60	0.17	1.3	2.4	—	0.54	2.7
$(P_l^-, P_l^+) = (\mp 80\%, \pm 60\%)$	1.2	0.48	0.14	1.0	1.3	—	0.29	1.4
$(P_t^-, P_t^+) = (80\%, 60\%)$	1.5	0.60	0.17	1.3	2.1	2.0	0.39	2.8

Table 11: Same as Table 5, but for $\sqrt{s} = 800$ GeV and symmetry (c).

	$\mathrm{Re}\,g_4^\gamma$	$\mathrm{Re}\,g_4^Z$	$\mathrm{Re}\,\tilde{\lambda}_\gamma$	$\mathrm{Re}\,\tilde{\lambda}_Z$	$\mathrm{Re}\,\tilde{\kappa}_\gamma$	$\mathrm{Re}\,\tilde{\kappa}_Z$
no polarisation	4.1	3.4	1.1	0.92	4.5	3.3
$(P_l^-, P_l^+) = (\mp 80\%, 0)$	2.0	1.7	0.54	0.44	2.1	1.6
$(P_l^-, P_l^+) = (\mp 80\%, \pm 60\%)$	1.2	1.0	0.30	0.24	1.2	1.0
$(P_t^-, P_t^+) = (80\%, 60\%)$	1.8	1.6	0.28	0.23	1.9	1.5

Table 12: Same as Table 5, but for $\sqrt{s} = 800$ GeV and symmetry (d).

	$\mathrm{Im}\,g_4^\gamma$	$\mathrm{Im}\,g_4^Z$	$\mathrm{Im}\,\tilde{\lambda}_\gamma$	$\mathrm{Im}\,\tilde{\lambda}_Z$	$\mathrm{Im}\,\tilde{\kappa}_\gamma$	$\mathrm{Im}\,\tilde{\kappa}_Z$
no polarisation	3.8	2.8	0.72	0.60	4.0	2.9
$(P_l^-, P_l^+) = (\mp 80\%, 0)$	1.6	1.3	0.34	0.28	1.8	1.4
$(P_l^-, P_l^+) = (\mp 80\%, \pm 60\%)$	0.93	0.79	0.19	0.16	1.1	0.86
$(P_t^-, P_t^+) = (80\%, 60\%)$	1.7	1.3	0.25	0.21	1.7	1.4

Table 13: Averages over the absolute values of the off-diagonal elements in the correlation matrices (27) in %, for symmetry (a) with $\sqrt{s} = 500$ GeV and different beam polarisations. Apart from the average over all 28 couplings (last column) we list the averages over the correlations between L-couplings (LL), between R-couplings (RR) and those between one L- and one R-coupling (LR).

	LL	RR	LR	all
no polarisation	22	42	14	22
$(P_l^-, P_l^+) = (\mp 80\%, 0)$	22	41	4	16
$(P_l^-, P_l^+) = (\mp 80\%, \pm 60\%)$	22	37	2	13
$(P_t^-, P_t^+) = (80\%, 60\%)$	20	26	8	15

A Appendix: Phase conventions of the helicity states

To make the discrete symmetry properties of the initial state (cf. Sect. 3) more apparent, we present in detail our phase conventions of the helicity states in this appendix. The resulting criteria for CP and $RCP\tilde{T}$ invariance of the spin density matrix are shown in Appendix B. Our starting point is a Wigner basis of electron and positron states (see Chapter 16 of [19]) defined in the e^-e^+ c.m. system:

$$|e^-(\mathbf{p}, \sigma)\rangle_{\mathrm{W}}, \qquad |e^+(\mathbf{p}, \sigma)\rangle_{\mathrm{W}} \qquad (\sigma = \pm 1). \tag{29}$$

Here $\mathbf{p}$ is an arbitrary three-momentum in the e^-e^+ c.m., given in the coordinate system fixed by the $e^-e^+ \to W^-W^+$ scattering plane (cf. Fig. 1), and $\sigma/2$ is the spin component along the positive z-axis (we follow the notation of [8] and normalise all spin and helicity indices to 1). We set

$$\mathbf{k}_\pm := (0, 0, \pm|\mathbf{k}|), \qquad |\mathbf{k}| = \frac{1}{2}\sqrt{s - 4m_e^2}\,, \tag{30}$$

where $\sqrt{s}$ is the c.m. energy of e^-e^+. We define the helicity states with momentum $\mathbf{k}_+$ to be the Wigner states

$$|e^\pm(\mathbf{k}_+, \tau)\rangle_{\mathrm{H}} = |e^\pm(\mathbf{k}_+, \tau)\rangle_{\mathrm{W}}. \tag{31}$$

We define the helicity states with momentum $\mathbf{k}_-$ by a rotation of $+\pi$ around the y-axis, i.e. we set

$$R = \exp(-i\pi J_y), \qquad |e^\pm(\mathbf{k}_-, \tau)\rangle_{\mathrm{H}} = U(R)|e^\pm(\mathbf{k}_+, \tau)\rangle_{\mathrm{H}}, \tag{32}$$

where J_y is the angular momentum along y. The transformation formulae for the Wigner states (see Appendix J, 16.3 of [19]) give

$$|e^\pm(\mathbf{k}_-, \tau)\rangle_{\mathrm{H}} = -|e^\pm(\mathbf{k}_-, \sigma)\rangle_{\mathrm{W}}\ \ \epsilon_{\sigma\tau} \tag{33}$$

with

$$\epsilon = \begin{pmatrix} 0 & 1 \\ -1 & 0 \end{pmatrix} . \tag{34}$$

Here and in the following summation over repeated indices is understood. Our sign convention in the exponent of (32) together with the prescription to rotate around $\hat{\boldsymbol{e}}_{\boldsymbol{y}}$ by +180 degrees is consistent with the spinors[5] (103) and (104) of [8]. For the spin density matrix $\boldsymbol{\rho}$ of the e^-e^+ system in the helicity and Wigner bases we obtain the relation

$$\begin{aligned} &{}_{\mathrm{H}}\Big\langle e^-(\mathbf{k}_+,\tau)e^+(\mathbf{k}_-,\overline{\tau})\Big|\,\boldsymbol{\rho}\,\Big|e^-(\mathbf{k}_+,\tau')e^+(\mathbf{k}_-,\overline{\tau}')\Big\rangle_{\mathrm{H}} \\ &\qquad = {}_{\mathrm{W}}\Big\langle e^-(\mathbf{k}_+,\tau)e^+(\mathbf{k}_-,\overline{\sigma})\Big|\,\boldsymbol{\rho}\,\Big|e^-(\mathbf{k}_+,\tau')e^+(\mathbf{k}_-,\overline{\sigma}')\Big\rangle_{\mathrm{W}}\ \epsilon_{\overline{\sigma}\,\overline{\tau}}\ \epsilon_{\overline{\sigma}'\overline{\tau}'}\ , \end{aligned} \tag{35}$$

or, in shorthand notation,

$$\rho^{\mathrm{H}}_{(\tau\overline{\tau})(\tau'\overline{\tau}')} = \rho^{\mathrm{W}}_{(\tau\overline{\sigma})(\tau'\overline{\sigma}')}\ \epsilon_{\overline{\sigma}\,\overline{\tau}}\ \epsilon_{\overline{\sigma}'\overline{\tau}'}\ , \tag{36}$$

where ρ^{H} is the spin density matrix in the helicity basis and ρ^{W} is the one in the Wigner basis. The matrix ρ^{H} is therefore the same as ρ in (5). If the spin density matrix in the Wigner basis factorises, i.e. if

$$\rho^{\mathrm{W}}_{(\tau\overline{\tau})(\tau'\overline{\tau}')} = \rho^{\mathrm{W}}_{\tau\tau'}\ \overline{\rho}^{\mathrm{W}}_{\overline{\tau}\,\overline{\tau}'}\ , \tag{37}$$

it also factorises in the helicity basis, with factors

$$\rho^{\mathrm{H}}_{\tau\tau'} = \rho^{\mathrm{W}}_{\tau\tau'}\ , \qquad \overline{\rho}^{\mathrm{H}}_{\overline{\tau}\,\overline{\tau}'} = \overline{\rho}^{\mathrm{W}}_{\overline{\sigma}\,\overline{\sigma}'}\ \epsilon_{\overline{\sigma}\,\overline{\tau}}\ \epsilon_{\overline{\sigma}'\overline{\tau}'}\ . \tag{38}$$

We parameterise ρ^{W} and $\overline{\rho}^{\mathrm{W}}$ as usual:

$$\rho^{\mathrm{W}}_{\tau\tau'} = \frac{1}{2}\left(\mathbb{1} + \vec{p}^{\,-}\cdot\vec{\sigma}\right)_{\tau\tau'}\ , \qquad \overline{\rho}^{\mathrm{W}}_{\overline{\tau}\,\overline{\tau}'} = \frac{1}{2}\left(\mathbb{1} + \vec{p}^{\,+}\cdot\vec{\sigma}\right)_{\overline{\tau}\,\overline{\tau}'}\ , \tag{39}$$

where $\vec{p}^{\,\pm}$ are the vectors defined in (15). This results in the following form of the spin density matrices in the helicity basis:

$$\rho^{\mathrm{H}}_{\tau\tau'} = \frac{1}{2}\left(\mathbb{1} + \vec{p}^{\,-}\cdot\vec{\sigma}\right)_{\tau\tau'}, \qquad \overline{\rho}^{\mathrm{H}}_{\overline{\tau}\,\overline{\tau}'} = \frac{1}{2}\left(\mathbb{1} - \vec{p}^{\,+}\cdot\vec{\sigma}^{*}\right)_{\overline{\tau}\,\overline{\tau}'}, \tag{40}$$

as given in (14).

[5] Note that, compared with the coordinate system used here, the spinors in [8] are defined in a system rotated by Θ around the y-axis.

B Appendix: CP and $RCP\tilde{T}$ invariance of the initial state

For a symmetry operation that is defined by a unitary operator U acting on the space of state vectors, invariance of $\boldsymbol{\rho}$ under this symmetry is expressed as

$$\boldsymbol{\rho} = U^\dagger \boldsymbol{\rho}\, U. \tag{41}$$

We have to reformulate this matrix equation in component notation in the helicity basis for the symmetries CP and $RCP\tilde{T}$. The transformation of the Wigner states under CP is defined by the unitary operator [19]

$$U(CP)|e^\pm(\mathbf{p},\sigma)\rangle_{\mathrm{W}} = \mp|e^\mp(-\mathbf{p},\sigma)\rangle_{\mathrm{W}}. \tag{42}$$

Hence, for an e^-e^+ state in the helicity basis we have

$$U(CP)|e^-(\mathbf{k}_+,\tau)e^+(\mathbf{k}_-,\overline{\tau})\rangle_{\mathrm{H}} = -|e^-(\mathbf{k}_+,\overline{\sigma})e^+(\mathbf{k}_-,\sigma)\rangle_{\mathrm{H}}\ \epsilon_{\overline{\sigma}\,\overline{\tau}}\,\epsilon_{\sigma\tau}\ , \tag{43}$$

where the sign due to the interchange of fermions is taken into account. Invariance of $\boldsymbol{\rho}$ under CP then corresponds to:

$$\rho^{\mathrm{H}}_{(\tau\overline{\tau})(\tau'\overline{\tau}')} = \rho^{\mathrm{H}}_{(\overline{\sigma}\sigma)(\overline{\sigma}'\sigma')}\ \epsilon_{\overline{\sigma}\,\overline{\tau}}\ \epsilon_{\sigma\tau}\ \epsilon_{\overline{\sigma}'\overline{\tau}'}\ \epsilon_{\sigma'\tau'}\ , \tag{44}$$

which leads to the conditions (24) on the polarisation parameters.

We define the discrete symmetry $\tilde{T}$ by a *unitary* operator that acts on the Wigner states as follows:

$$U(\tilde{T})|e^\pm(\mathbf{p},\sigma)\rangle_{\mathrm{W}} = -|e^\pm(-\mathbf{p},\sigma')\rangle_{\mathrm{W}}\ \epsilon_{\sigma'\sigma}\ . \tag{45}$$

For the combined symmetry $U(CP\tilde{T}) = U(CP)U(\tilde{T})$ we then obtain

$$U(CP\tilde{T})|e^\pm(\mathbf{k}_\mp,\tau)\rangle_{\mathrm{H}} = \pm|e^\mp(\mathbf{k}_\mp,\tau')\rangle_{\mathrm{H}}\ \epsilon_{\tau'\tau}\ . \tag{46}$$

Together with a subsequent rotation around the y-axis by $+180$ degrees (32) we have

$$U(RCP\tilde{T})|e^\pm(\mathbf{k}_\mp,\tau)\rangle_{\mathrm{H}} = -|e^\mp(\mathbf{k}_\pm,\tau')\rangle_{\mathrm{H}}\ \epsilon_{\tau'\tau}\ . \tag{47}$$

The transformation of the combined e^-e^+ state is then

$$U(RCP\tilde{T})|e^-(\mathbf{k}_+,\tau)e^+(\mathbf{k}_-,\overline{\tau})\rangle_{\mathrm{H}} = -|e^-(\mathbf{k}_+,\overline{\sigma})e^+(\mathbf{k}_-,\sigma)\rangle_{\mathrm{H}}\ \epsilon_{\overline{\sigma}\,\overline{\tau}}\ \epsilon_{\sigma\tau}\ , \tag{48}$$

where again the interchange of two fermions is taken into account. Invariance of $\boldsymbol{\rho}$ under $RCP\tilde{T}$ then again leads to (44). So, as for CP, *full* invariance of $\boldsymbol{\rho}$ requires (24), whereas invariance of the *reduced* matrix $\tilde{\boldsymbol{\rho}}$ (26) is trivially fulfilled.

References

[1] "TESLA Technical Design Report Part I: Executive Summary," eds. F. Richard, J. R. Schneider, D. Trines and A. Wagner, DESY, Hamburg, 2001 [hep-ph/0106314];
"TESLA Technical Design Report Part III: Physics at an e^+e^- Linear Collider," eds. R.-D. Heuer, D. Miller, F. Richard, P. M. Zerwas, DESY, Hamburg, 2001 [hep-ph/0106315].

[2] J. R. Ellis, E. Keil and G. Rolandi, CERN-EP-98-03;
J. P. Delahaye *et al.*, in: *Proc. of the 20th Intl. Linac Conference LINAC 2000* ed. Alexander W. Chao, eConf C000821, MO201 (2000) [physics/0008064].

[3] K. Hagiwara, R. D. Peccei, D. Zeppenfeld and K. Hikasa, Nucl. Phys. B **282**, 253 (1987).

[4] M. Suzuki, Phys. Lett. B **153**, 289 (1985);
G. Couture and J. N. Ng, Z. Phys. C **35**, 65 (1987);
T. G. Rizzo and M. A. Samuel, Phys. Rev. D **35**, 403 (1987);
G. Couture, J. N. Ng, J. L. Hewett and T. G. Rizzo, Phys. Rev. D **36**, 859 (1987);
X. G. He and B. H. McKellar, Phys. Rev. D **42**, 3221 (1990) [Erratum-ibid. D **50**, 4719 (1994)];
A. J. Davies, G. C. Joshi and R. R. Volkas, Phys. Rev. D **42**, 3226 (1990);
D. Atwood, C. P. Burgess, C. Hamazaou, B. Irwin and J. A. Robinson, Phys. Rev. D **42**, 3770 (1990);
D. Chang, W. Y. Keung and J. Liu, Nucl. Phys. B **355**, 295 (1991);
T. G. Rizzo, Phys. Rev. D **46**, 3894 (1992) [hep-ph/9205207];
X. G. He, J. P. Ma and B. H. McKellar, Phys. Lett. B **304**, 285 (1993) [hep-ph/9209260];
A. Sugamoto, Phys. Lett. B **354**, 363 (1995) [hep-ph/9501236];
A. Arhrib, J. L. Kneur and G. Moultaka, Phys. Lett. B **376**, 127 (1996) [hep-ph/9512437];
E. N. Argyres, A. B. Lahanas, C. G. Papadopoulos and V. C. Spanos, Phys. Lett. B **383**, 63 (1996) [hep-ph/9603362];
F. Larios, J. A. Leyva and R. Martinez, Phys. Rev. D **53**, 6686 (1996);
N. K. Sharma, P. Saxena, S. Singh, A. K. Nagawat and R. S. Sahu, Phys. Rev. D **56**, 4152 (1997);
G. Tavares-Velasco and J. J. Toscano, Phys. Rev. D **65**, 013005 (2002) [hep-ph/0108114].

[5] W. Kilian, hep-ph/0303015;
K. Mönig, hep-ph/0303023.

[6] A. Heister *et al.* [ALEPH Collaboration], Eur. Phys. J. C **21**, 423 (2001) [hep-ex/0104034];
P. Abreu *et al.* [DELPHI Collaboration], Phys. Lett. B **459**, 382 (1999);
M. Acciarri *et al.* [L3 Collaboration], Phys. Lett. B **467**, 171 (1999) [hep-ex/9910008]; Phys. Lett. B **487**, 229 (2000) [hep-ex/0007005];
G. Abbiendi *et al.* [OPAL Collaboration], Eur. Phys. J. C **19**, 1 (2001) [hep-ex/0009022]; Eur. Phys. J. C **19**, 229 (2001) [hep-ex/0009021].

[7] G. Moortgat-Pick and H. Fraas, Acta Phys. Polon. B **30**, 1999 (1999) [hep-ph/9904209];
G. Moortgat-Pick, A. Bartl, H. Fraas and W. Majerotto, Eur. Phys. J. C **18**, 379 (2000) [hep-ph/0007222];
G. Moortgat-Pick and H. M. Steiner, Eur. Phys. J. direct C **3**, 6 (2001) [hep-ph/0106155];
J. Erler *et al.*, in *Proc. of the APS/DPF/DPB Summer Study on the Future of Particle Physics (Snowmass 2001)* ed. N. Graf, eConf **C010630**, E3004 (2001) [hep-ph/0112070];
C. Blochinger, H. Fraas, G. Moortgat-Pick and W. Porod, Eur. Phys. J. C **24**, 297 (2002) [hep-ph/0201282];
G. Moortgat-Pick, hep-ph/0303234.

[8] M. Diehl, O. Nachtmann and F. Nagel, Eur. Phys. J. C **27**, 375 (2003) [hep-ph/0209229].

[9] G. Alexander et al., SLAC-Proposal-E-166, Stanford, 2003.

[10] *http://www.ippp.dur.ac.uk/˜gudrid/power/.*

[11] J. Fleischer, K. Kolodziej and F. Jegerlehner, Phys. Rev. D **49**, 2174 (1994).

[12] D. Zeppenfeld, Phys. Lett. B **183**, 380 (1987).

[13] K. Hagiwara *et al.* [Particle Data Group Collaboration], Phys. Rev. D **66**, 010001 (2002).

[14] M. Diehl and O. Nachtmann, Z. Phys. C **62**, 397 (1994).

[15] S. Alam, Phys. Rev. D **50**, 174 (1994);
A. Arhrib, J. L. Kneur and G. Moultaka, Phys. Lett. B **376**, 127 (1996) [hep-ph/9512437];
K. P. Diener, B. A. Kniehl and A. Pilaftsis, Phys. Rev. D **57**, 2771 (1998) [hep-ph/9709361];
A. A. Barrientos Bendezu, K. P. Diener and B. A. Kniehl, Phys. Lett. B **478**, 255 (2000) [hep-ph/0002058];
S. Alam, K. Hagiwara, S. Kanemura, R. Szalapski and Y. Umeda, Phys. Rev. D

62, 095011 (2000) [hep-ph/0002066];
T. Hahn, Nucl. Phys. B **609**, 344 (2001) [hep-ph/0007062].

[16] M. Diehl and O. Nachtmann, Eur. Phys. J. C **1**, 177 (1998) [hep-ph/9702208].

[17] D. Atwood and A. Soni, Phys. Rev. D **45**, 2405 (1992);
M. Davier, L. Duflot, F. Le Diberder and A. Rougé, Phys. Lett. B **306**, 411 (1993).

[18] W. Menges, Linear Collider Note LC-PHSM-2001-022.

[19] O. Nachtmann, "Elementary particle physics: concepts and phenomena", Springer Verlag, Berlin, Heidelberg, 1990.